Journal of Electrostatics 89 (2017) 20–29

Contents lists available at ScienceDirect

Journal of Electrostatics

journal homepage: www.elsevier.com/locate/elstat

# Capacitance and forces for two square electrodes

Francesco Maccarrone [a, *], Giampiero Paffuti [b]

[a] University of Pisa, Physics Department, Largo Pontecorvo 7, Pisa, Italy
[b] University of Pisa, Physics Department and INFN Pisa, Largo Pontecorvo 7, Pisa, Italy

ARTICLE INFO

*Article history:*
Received 1 June 2017
Received in revised form
27 June 2017
Accepted 28 June 2017

*Keywords:*
Coefficients of capacitance
Asymptotic formulas for capacitance
Force in square capacitor

ABSTRACT

A numerical and semi-analytical study of electrostatics of a system of two parallel square electrodes is focused on the behavior at short and large distances of the capacity coefficients and of the electrostatic forces between the plates. It is found, using a Boundary Element Method approach with a regular grid and an analytical treatment of the kernel matrix, a strict parallelism with the analogous system of two circular disks, in particular for the possibility of disentangle the divergences at short distances and the presence of a logarithmically divergent repulsive force, with the exception of electrodes with exactly opposite charges. With our semi-analytical approach, fully exploiting the symmetries of the problem and using very small subdomains, the capacitance coefficients of the two square capacitor are determined with a great accuracy, comparable with the best data available in the literature just for the capacitance of a single square.



## 1. Introduction

Recently, the classical problem of electrostatic forces between two conductors at close approach has been the object of several investigations [1,2]. In Ref. [3] it has been noted that two conducting spheres brought close enough attract each other, except in special cases, while in Refs. [4,5] it has been shown that two disks tend to repel each other and that the force is logarithmic divergent for equal disks. In both cases the effects are due to a charge redistribution and in Refs. [4,5] we conjectured that the alternative behavior depends on the dimension of the nearly-contact zone and on the superposition of edges. On general grounds, the forces can be deduced from capacitance coefficients and a particular linear combination of these coefficients has been proposed in Ref. [6] to distinguish the different divergent behaviours at short distances. The opposite regime of large distances has also some interest. It has been pointed out in Ref. [7] that in this regime the leading terms of the dependence of the coefficients of capacitance on the distance are directly related to a few physical parameters of the separated conductors: self-capacitance, quadrupole moment and polarizability. The interest of those general relations is in the possibility of measuring these intrinsic parameters by large distance experiments.

Unfortunately, only few systems can be analytically studied and to enlarge our understanding of the problems it is necessary to use approximate methods. This work is a first step in this direction dealing with the paradigmatic case of two parallel square electrodes. It is well known that an exact solution is lacking and only numerical and semi-analytical studies of the electrostatic problem for two equal square parallel electrodes are available. In this paper we study numerically this system, starting from a semi-analytical position of the electrostatic problem.

Among the many numerical schemes both deterministic [8,9] and stochastic [10] we choose the Boundary Element Method which is clearly and shortly outlined in a recent paper of Read and Bowring [11]. Generally speaking, the surfaces of the conductors are divided into subareas, the charge onto each element is assumed uniform and the electrostatic problem is converted into a linear algebraic system. The choice of BEM is quite natural for its simplicity but we avoid the use of collocation points algorithms as they can introduce distortions in the computation at small separation and because they are not based on a variational principle. We overcome these problems by adopting a kernel integrated *both* on the initial and final elementary domains. The integrals are done analytically for square plaquettes and this provides both a variational approach and frees the calculation from inevitable errors in the numerical evaluation of the integrals. The choice of square as elementary domains is partly dictated by the availability of the analytical form of the integrals, and partly to the possibility of using the symmetry properties of the problem to reduce the size of the

* Corresponding author.
*E-mail address:* francesco.maccarrone@unipi.it (F. Maccarrone).

http://dx.doi.org/10.1016/j.elstat.2017.06.007
0304-3886/

matrices. The method could be generalized by using a finer grid near the edges of the square [12] or by using a triangular tessellation which is more flexible in the coverage of a plane surface and for which some analytical results are known [13]. The discussion of these alternative algorithms is beyond our scope which is not to write an optimized code but to have an algorithm under control. With the scheme used the accuracy of the given results is aligned with the best data available in the literature [14,15] for the capacitance of a single square. Moreover, they provide a novel numerical estimation of similar accuracy for the capacitance coefficients of the two squares capacitor, also for very small aspect ratios.

The focus of this work is on the behavior at large and short distances. In particular, we look for the edge corrections of selected capacitance coefficients, as these play a major role in fixing the forces at short distance. The results at long distance confirm the general expansion in terms of the physical properties of the electrodes, i.e. the self-capacitance and the quadrupole moment. We also show that the same expansion can be used as an effective tool to obtain directly these quantities from numerical estimation of capacitance coefficients.

In the short distance regime we found a strict parallelism with the behavior of the similar system composed by two circular electrodes, in particular for short distances $s$ a correction proportional to $s\log s$ appears in the global capacitance $C_{g_1} = C_{11} + C_{12}$: this term is responsible of a repulsive force between the electrodes, in the generic case. The effect is explained by the redistribution of the charges and the enhancement of their density at the edges.

More problematic is the study of the edge corrections to the usual mutual capacitance, given by $C = (C_{11} - C_{12})/2$. At a qualitative level we show that it is present a $\log s$ correction, but a definite identification with the usual Thomson approximation is out of reach due to the limited accuracy of the feasible numerical computation.

The paper is organized as follows. In section 2 we outline the frame of our computation. In section 3 we give the details of the numerical method used and section 4 contains the results. Sections 5 and 6 are devoted to the analysis of large and short distances regimes respectively. Section 7 contains a brief description of the forces deduced from the above calculations.

## 2. Outline of the computation

The capacitance coefficients $C_{ij}$ are the elements of a symmetric matrix and for a system of conductors they are defined by

$$Q_i = \sum_j C_{ij} V_j; \quad C_{ji} = C_{ij} \tag{1}$$

where $Q_i, V_i$ are the charge and the potential of the $i$-th conductor, respectively. The coefficients $C_{ij}$ depend only on the geometry of the system. It is also useful to consider the matrix of potential coefficients, with elements $M_{ij}$, defined as the inverse matrix of $C_{ij}$. In terms of these coefficients the electrostatic energy of the system is written as

$$W = \frac{1}{2} \sum_{i,j} M_{ij} Q_i Q_j. \tag{2}$$

In this work we limit ourselves to a particular system: two square plates with side $L$. The first square is placed in the $x, y$ plane and the second is obtained by a translation of length $s$ along the $z$ axis: the geometric parameters are $L$ and $s$ and $C_{ij}$ depend only on these variables. In the following we use Gaussian units to simplify the notation. The coefficients $C_{ij}$ are proportional to a length, then by dimensional analysis

$$C_{ij}(L, s) = L C_{ij}(1, s/L). \tag{3}$$

Equation (3) reduce the problem to the study of the system with $L = 1$ and the only remaining variable is the dimensionless quantity $\kappa = s/L$. For two equal squares, symmetry implies $C_{11} = C_{22}$, then we have only two independent quantities, $C_{11}$ and $C_{12}$ or two linearly independent combinations of them.

In the following we follow the strategy outlined in Ref. [6] and we adopt as variables the combinations

$$C_{g_1} = C_{11} + C_{12}\ ; \quad C = \frac{C_{11} - C_{12}}{2} \tag{4}$$

The coefficient $C$ is the usual mutual capacitance, i.e. the charge on each plate in the case $V_1 = -V_2$. In the general case it is convenient to define $C_g$, the *global capacitance* of the system, defined as the total charge of the system when both electrodes are kept at unit potential:

$$Q_1 + Q_2 = C_g V. \tag{5}$$

$C_{g_1}$ is the charge on one plate for unit potentials, and for equal electrodes it follows by symmetry:

$$C_{g_1} = C_g/2. \tag{6}$$

In terms of these parameters the energy (2) takes the form

$$W = \frac{1}{4} \frac{(Q_1 + Q_2)^2}{C_{g_1}} + \frac{1}{8} \frac{(Q_1 - Q_2)^2}{C} \tag{7}$$

The decomposition (4) allows a clear distinction in the short distance behavior. For a couple of squares the limit of $C$ at vanishing distance is

$$C \underset{s\to 0}{\to} \frac{1}{4\pi} \frac{Area}{s} (1 + \mathcal{O}(s \log s)) = \frac{L}{4\pi\kappa} (1 + \mathcal{O}(\kappa \log \kappa)) \equiv C_{geom} (1 + \mathcal{O}(\kappa \log \kappa)) \tag{8}$$

while $C_g$ approaches the global capacitance of the superimposed squares, i.e. a single square of side $L$, denoted by $C_1$ in the following:

$$C_g \underset{s\to 0}{\to} C_1; \quad C_{g_1} \underset{s\to 0}{\to} \frac{C_1}{2}. \tag{9}$$

Scaling considerations analogous to (3) allow to put $L = 1$ and, once computed $C_1$ for this value, we know $C_1$ for every $L$: $C_1[L] = L\, C_1[1]$.

At large distances the natural combinations are $C_{11}$ and $C_{12}$, as it is well known that, at the leading order

$$C_{11} \underset{d\to\infty}{\to} C_1; \quad C_{12} \to 0. \tag{10}$$

A more complete large distance expansion is given below, in equation (36). It is worth noting that the same parameter, $C_1$, determines both the short distance behavior of $C_g$ and the long distance behavior of $C_{11}$.

The knowledge of the large distance expansion (36) requires the computation on a single plate to estimate directly $C_1$ and the quadrupole moment.

A second more demanding computation on the system of two plates at different distances is required to give an estimate of the corrections to (8) and (9). These corrections are needed to compute the forces between electrodes at short distances. The force can be

calculated as $-\partial W/\partial s$ at fixed charges:

$$F = \frac{1}{4}\frac{(Q_1+Q_2)^2}{C_{g_1}^2}\frac{\partial}{\partial s}C_{g_1} + \frac{1}{8}\frac{(Q_1-Q_2)^2}{C^2}\frac{\partial}{\partial s}C. \tag{11}$$

From (8) it follows that the second term in (11) contributes to the force between the square electrodes with a attractive term independent of s. Then, for the short distance behavior of $F$ it is crucial to know the next order term in (9). If a better knowledge of capacitance is required, independently of forces, we need also the next order in (8). These corrections are usually referred to as *edge effects*.

## 3. Numerical method

The general electrostatic problem for conductors can be reduced to the computation of the charge distribution on the electrodes at fixed potentials. Here, the capacitance coefficients are computed by a variant of the Boundary Elements Method (BEM), approximating the distributions by piecewise constant functions.

Let us explain in details our approach in the case of a single conductor. The surface $S$ of the body is divided into cells of area $A_i$ and charge $q_i$. The electrostatic problem is approximated by

$$\sum_j K_{ij} q_j = V_i \tag{12}$$

where $V_i$ is constant (i.e. independent of $i$) and $K_{ij}$ the interaction kernel between the cells $i$ and $j$. Solving the linear system (12) for $V_i = 1$ fixes the charges $q_i$ and the capacity in this approximation is given by

$$C_{BEM} = \sum_i q_i. \tag{13}$$

The various implementations of BEM differ by the choice of $K_{ij}$. Our choice is to consider the charges $q_i$ uniformly distributed on each plaquette, of area $A_i$. The resulting $K_{ij}$ is given by

$$K_{ij} = \frac{1}{A_i}\frac{1}{A_j}\int\limits_{\mathbf{x}\in A_i}\int\limits_{\mathbf{y}\in A_j}\frac{1}{|\mathbf{x}-\mathbf{y}|} \equiv \frac{1}{A_i A_j}\tilde{K}_{ij} \tag{14}$$

The explicit expression for $\tilde{K}_{ij}$ in the case of rectangular subareas is given in A. The adopted procedure is not the simplest one but it has a simple interpretation in terms of variational methods, at least for conductors with piecewise planar surfaces.

Let us consider an arbitrary charge distribution $\sigma(\mathbf{x})$ on the surface $S$, the actual distribution on a conductor corresponds to the minimum of the energy functional

$$\mathscr{E} = \frac{1}{2}\int\limits_{\mathbf{x}\in S}\int\limits_{\mathbf{y}\in S}\frac{\sigma(\mathbf{x})\sigma(\mathbf{y})}{|\mathbf{x}-\mathbf{y}|} \tag{15}$$

for a given total charge $Q$. At the minimum the energy is given by

$$\mathscr{E}_0 = \min(\mathscr{E}) = \frac{1}{2}\frac{Q^2}{C} \tag{16}$$

$Q$ is the *total charge* on the conductor and $C$ its capacity, related to the constant potential acquired by the conductor by $Q = VC$. Consider now a partition of $S$ in elements $S_i$ with area $A_i$, $i = 1\ldots N_P$, and a corresponding piecewise constant distribution $\sigma(\mathbf{x}) = \sigma_i$ for $\mathbf{x}\in S_i$. The energy functional (15) reduces to

$$\mathscr{E} = \sum_{i,j}\frac{1}{2}\sigma_i\sigma_j\int\limits_{\mathbf{x}\in S_i}\int\limits_{\mathbf{y}\in S_j}\frac{1}{|\mathbf{x}-\mathbf{y}|} \equiv \sum_{i,j}\frac{1}{2}\sigma_i\sigma_j\tilde{K}_{ij} \tag{17}$$

The minimum of this functional under the constraint of fixed charge can be obtained introducing a Lagrange multiplier $\lambda$ and the equation for the minimum takes the form

$$\frac{\partial}{\partial\sigma_i}\left(\mathscr{E} - \lambda\sum_j \sigma_j A_j\right) = 0 \Rightarrow \sum_j \tilde{K}_{ij}\sigma_j = \lambda A_i \tag{18}$$

where $\lambda$ is fixed by the requirement $\sum_i \sigma_i A_i = Q$. Substituting in (17) and using the definition of minimum energy

$$\mathscr{E} = \sum_i \frac{1}{2}\sigma_i\lambda A_i = \frac{1}{2}Q\lambda \geq \frac{Q^2}{2C} \Rightarrow \frac{Q}{\lambda} \leq C. \tag{19}$$

With the change of variables

$$\sigma_i = \frac{1}{A_i}q_i\lambda$$

equation (18) reads

$$\sum_j \frac{1}{A_i A_j}\tilde{K}_{ij}q_j = 1, \tag{20}$$

i.e. (12) for $V_i = 1$, and the bound (19) becomes

$$\sum_i q_i = C_{BEM} \leq C. \tag{21}$$

The inequality (21) implies that a discretization with $N_P$ cells gives a lower bound for the true $C$. Moreover, as $N_P$ grows, the approximation to $C$ is monotone, as a consequence of the variational method.

We have exposed the BEM method in the case of a single conductor but the procedure, and the connection with the variational method, is easily extended to more general cases. In this paper we intend to calculate the capacitance coefficients for two equal and parallel square plates. In the configuration with equal potentials $V$, and then, for equal plates, with equal charges $Q$ and total charge $2Q$, the energy has the form

$$\mathscr{E}_0 = \frac{1}{2}\frac{(2Q)^2}{C_g} = \frac{Q^2}{C_{g_1}} \tag{22}$$

where

$$C_g = (C_{11} + C_{22} + 2C_{12}) = 2(C_{11} + C_{12}) \equiv 2C_{g_1} \tag{23}$$

In the linear system (20) the sum runs over all the $2N_P$ subareas for two squares equally subdivided as in the single conductor case.

For the configuration with opposite charges the energy has the usual expression

$$\mathscr{E}_0 = \frac{1}{2}\frac{Q^2}{C} \tag{24}$$

where $C = (C_{11} - C_{12})/2$ is the mutual capacitance. In this case the right-hand term in (20) take the values 1 for the first plate and $-1$ for the second.

Each plate is covered by $N_P = N^2$ cells and the matrix $K_{ij}$ has a size $(2N_P)\times(2N_P) = 4N^4$, then for large $N$ memory occupation is a

problem. Symmetry considerations can help. For the computation of $C_{g_1}$ and $C$ we have to solve (12) with a vector $V$ of the symbolic form $(1,1)$ and $(1,-1)$ respectively, each entry having length $N_P$. Symmetry ensures also that in the two cases the two vectors of charge distribution on the two plaquettes are equal or opposite respectively. The system (12) takes the form

$$\begin{pmatrix} A & B \\ B & A \end{pmatrix} \begin{pmatrix} q \\ \pm q \end{pmatrix} = \begin{pmatrix} 1 \\ \pm 1 \end{pmatrix} \tag{25}$$

where the sub-matrices $A, B$ are the matrix elements $K_{ij}$ for a plate with itself and with the other plate, respectively. The two computations are then reduced to the solution of the two $N_P \times N_P$ systems

$$(A+B)q_1 = 1; \quad (A-B)q_2 = 1. \tag{26}$$

The sum of the components of the resulting vector solutions gives

$$\begin{aligned} C_{g_1} &= C_{11} + C_{12} = \sum q_1 \\ C &= \frac{C_{11} - C_{12}}{2} = \frac{1}{2}\sum q_2 \end{aligned} \tag{27}$$

A further factor can be gained by noticing that, from the symmetry of the squares, each plate can be divided in four equivalent quadrants, then the matrices $A, B$ can be in effect reduced to the size $(N_P/4) \times (N_P/4)$. The decomposition of the matrices like $K$ in two submatrices $A, B$ for two equal squares has already been noted in Ref. [16].

The implementation of the numerical scheme solving the linear systems (26) requires the explicit expression of $\bar{K}_{ij}$, given in Appendix A.

## 4. Numerical results

The method exposed in section 3 has been applied to the problem of two parallel square plates $L \times L$ with $L = 1$. We choose to work with a grid of square plaquettes $(2dx) \times (2dx)$ with $2dx = L/N$, i.e. $N_P = N^2$ elementary areas for each plate. A preliminary computation has been performed in order to fix the parameters of a single square. In this computation we used a series of $N$ up to 550, the final values of the parameters are obtained by extrapolating the numerical results with a polynomial of second degree in $1/N$ for $N \geq 250$. The results for the capacitance and the quadrupole moment are given in Table 1, together with a comparison with existing results obtained with smaller grids. Here and in the following we use Gaussian units for the capacitances and centimeters for the length. The conversion in SI units is straightforward multiplying our coefficient of capacitance by 1.11265 $10^{-12}$.

Another interesting feature for a single square is the behavior of the charge density near the edge. Near an edge on general grounds, see §3, §4 in Ref. [19], one expects

$$\sigma \sim a + b_\sigma \Big/ \sqrt{\xi}, \tag{28}$$

where $\xi$ is the distance from the edge. We found, for the distribution along the midline of the square

$$\sigma \simeq 0.041 + 0.222 \Big/ \sqrt{\xi}. \tag{29}$$

The charge density on the boundary of a square is not constant, due the presence of corners, then the actual value of $b_\sigma$ varies along the perimeter. In the following it will useful to have an estimate of the mean value of $b_\sigma^2$ along the perimeter. We found by avoiding the corners

$$\overline{b_\sigma^2} \simeq 0.066 \pm 0.002 \tag{30}$$

The main computation concerns the capacitance coefficients for two parallel squares at distance $s = \kappa L$. We computed through (27) the quantities

$$C_{g_1} = C_{11} + C_{12}; \quad C = \frac{C_{11} - C_{12}}{2}. \tag{31}$$

and $C_{11}$ and $C_{12}$ follow directly with

$$C_{11} = \frac{1}{2}C_{g_1} + C; \quad C_{12} = \frac{1}{2}C_{g_1} - C. \tag{32}$$

A short list of values is reported for reference in Table 2.

The computation has been performed for various $N$, up to $N = 460$ (for small $\kappa$) and the previous extrapolation procedure has been used to extract the final values. The limit on $N$ implies a limitation of order $\kappa \sim 1/N$ on the reliable distances and the results discussed below are based only on data obtained for $\kappa \geq 0.001$. We have verified that the numerical results are a growing function of $N$, as expected, following eq. (21) and the comment given after it. The values for $C$ at relatively large $\kappa$ are compatible with the literature, We are not aware of computations at small $\kappa$ for $C$ and in general of computations of $C_{g_1}$ and, through (32), of $C_{11}$ and $C_{12}$. Then, the data collected in Table 2 should be considered globally as an unprecedented result.

## 5. Large distance behavior

At large distances the capacitance coefficients for two conductors $a, b$ with the centres of charges separated by the vector $\mathbf{R}$ are

**Table 1**
Values of $C_1$ and quadrupole moment for a unit square.

| | $C_1$ | $D_{zz}$ |
|---|---|---|
| Goto et al. [17] | 0.3667892(11) | |
| Read [18] | 0.3667874(1) | |
| Read [15] | 0.3667896(8) | |
| Present result | 0.3667875(2) | −0.23010(2) |

**Table 2**
Values of $C_{g_1}$ and $C$ for some values of $\kappa = d/L$ and $L = 1$. Last column contains the values computed for $C$ in Ref. [16], with $N_{max} = 20$ and with a slightly different method.

| $\kappa$ | $C_{g1}$ | C | C(ref. [16]) |
|---|---|---|---|
| 7 | 0.348606 | 0.193485 | 0.193536 |
| 5 | 0.341930 | 0.197771 | 0.197823 |
| 3 | 0.327689 | 0.208241 | 0.208293 |
| 2 | 0.312404 | 0.222056 | 0.222107 |
| 1 | 0.280022 | 0.266026 | 0.266056 |
| 0.5 | 0.248085 | 0.355938 | 0.355840 |
| 0.2 | 0.218155 | 0.617821 | 0.616674 |
| 0.1 | 0.204338 | 1.039043 | 1.034348 |
| 0.09 | 0.202744 | 1.131364 | |
| 0.07 | 0.199383 | 1.393624 | |
| 0.05 | 0.195725 | 1.861898 | |
| 0.04 | 0.193748 | 2.269127 | |
| 0.03 | 0.191637 | 2.944683 | |
| 0.01 | 0.186762 | 8.300064 | |
| 0.009 | 0.186479 | 9.189246 | |
| 0.007 | 0.185895 | 11.727391 | |
| 0.005 | 0.185279 | 16.290441 | |
| 0.002 | 0.184265 | 40.201509 | |
| 0.001 | 0.183872 | 80.014327 | |
| 0.0007 | 0.183742 | 114.130158 | |

given by Ref. [7].

$$
\begin{aligned}
C_{11} &= C_1\left(1+\frac{C_1C_2}{R^2}\right.\\
&\left.+\frac{1}{R^4}\left(C_1^2C_2^2+C_1C_2D+C_1\alpha^{(2)}\right)\right)\\
C_{22} &= C_2\left(1+\frac{C_1C_2}{R^2}\right.\\
&\left.+\frac{1}{R^4}\left(C_1^2C_2^2+C_1C_2D+C_2\alpha^{(1)}\right)\right)\\
C_{12} &= C_{21} = -\frac{C_1C_2}{R}\left(1+\frac{D}{2R^2}+\frac{C_1C_2}{R^2}\right)
\end{aligned}
\tag{33}
$$

$C_1, C_2$ are the self capacitances, and

$$
\alpha^{(I)} = \alpha_{ij}^{(I)} n_i n_j; D = n_i n_j\left(D_{ij}^{(1)} + D_{ij}^{(2)}\right) \tag{34}
$$

where $\mathbf{n} = \mathbf{R}/R$. $\alpha_{ij}^{(I)}$ is the polarization tensor of the $I$-conductor and $D_{ij}^{(I)}$ is the quadrupole moment for unit charge of the $I$-conductor, defined by

$$
D_{ij}^{(I)} = \oint_{S_I}\left(3x_ix_j - x^2\delta_{ij}\right)\sigma(\mathbf{x})dA_x \tag{35}
$$

where $\sigma(\mathbf{x})$ is the charge density for the *isolated* conductor. For two equal and parallel squares $\mathbf{n}$ is the unit vector directed along the separation (the $z$ axis) and $C_{11} = C_{22}$. In this configuration only the components $\alpha_{zz}, D_{zz}$ contribute to (34). For two-dimensional squares clearly $\alpha_{zz} = 0$ then in (33) only the quadrupole term $D_{zz}$ contribute to the capacitance coefficients and $D = 2D_{zz}$. The resulting asymptotic behavior for capacitance coefficients as a function of $\kappa$ is (we use $L = 1$):

$$
\begin{aligned}
C_{11} &= C_1\left(1+\frac{C_1^2}{\kappa^2}+\frac{1}{\kappa^4}\left(C_1^4+2D_{zz}C_1^2\right)\right)\\
C_{12} &= -\frac{C_1^2}{\kappa}\left(1+\frac{1}{\kappa^2}\left(C_1^2+D_{zz}\right)\right)
\end{aligned}
\tag{36}
$$

The main feature of the result (36) is that for $\kappa\to\infty$, $C_{11}\to C_1$ and $C_{12}\to 0$. This is confirmed in Fig. 1.

A more quantitative check is obtained by subtracting the leading behavior for $\kappa\to\infty$:

$$
\Delta C_{11} = C_{11} - C_1\left(1+\frac{C_1^2}{\kappa^2}\right);\quad \Delta C_{12} = C_{12} + \frac{C_1^2}{\kappa}
$$

From (36) we expect, neglecting higher order in $1/\kappa$:

$$
\begin{aligned}
\Delta C_{11} &= \frac{C_1^3}{\kappa^4}\left(C_1^2+2D_{zz}\right);\\
\Delta C_{12} &= -\frac{C_1^2}{\kappa^3}\left(C_1^2+D_{zz}\right)
\end{aligned}
\tag{37}
$$

The numerical results are shown in Fig. 2. In Ref. [7] it has been pointed out that in principle the measurement of $C_{11}$ and $C_{12}$ at large distances allows the determination of the physical parameters for isolated conductors, in the present case $C_1$ and $D_{zz}$. We can verify this statement in our numerical computation. Fitting the computed values of $C_{12}$ at large distance with the form (36) we obtain the values listed in Table 3, in very good agreement with the values computed on the isolated square. Similar results, with a slightly lower precision, are obtained from $C_{11}$.

## 6. Short distance behavior

Two major difficulties arise in the study of the behavior of capacitance coefficients for $\kappa\to 0$, making it much more problematic than the large distance case. Firstly, the limitations on $N$ put a lower limit to computable $\kappa$'s, and on the theoretical side, the strong divergent behavior of $\sigma$ at the corners does not allow a simple analysis of the results. Even a refinement of the grid along the edges and at the corners, as suggested in Ref. [15], is not capable to manage the critical behavior of the BEM system at the lowest values of $\kappa$.

On general grounds, for $C_{g_1}$ and $C$ only the leading order (9), (8), for $s\to 0$ is known. We rewrite here, for readability, those expressions for $L = 1$:

$$
\lim_{\kappa\to 0} C_{g_1} = \frac{C_1}{2};\quad C \underset{\kappa\to 0}{\to} \frac{1}{4\pi}\frac{1}{\kappa}. \tag{38}
$$

### 6.1. $C_{g1}$ at close approach

The existence of the limits (38) implies a non trivial cancellation between the singularities in $C_{11}$ ad $C_{12}$. In Fig. 3 we show the approach to the limit of $C_{g1}$ in (38) obtaining a good agreement.

It is useful to recall that $C_g = 2C_{g_1}$ is the capacitance of the disconnected conductor composed by the two squares. In addition,

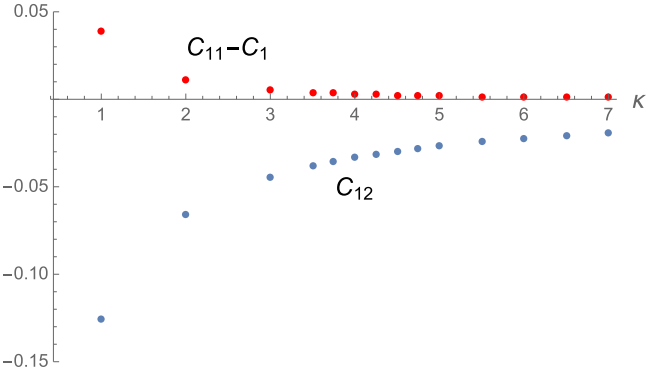


**Fig. 1.** Vanishing limits for $C_{11} - C_1$ and $C_{12}$ at large $\kappa$.

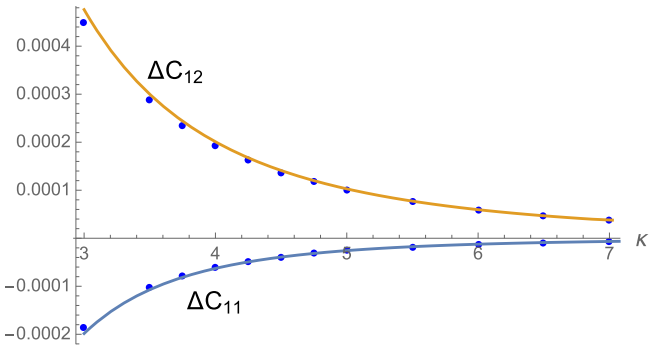


**Fig. 2.** Limit behavior of $\Delta C_{11}$ and $\Delta C_{12}$ (see (37)) for large $\kappa$. The points are the numerical results. The continuous lines are the graph of the expansions (37), using the computed parameters for the single plate given in Table 1.

**Table 3**
Parameters $C_1$ and $D_{zz}$ from the large $\kappa$ behavior of $C_{12}$.

| | $C_1$ | $D_{zz}$ |
|---|---|---|
| eq. (36) | 0.366774(2) | −0.2260(2) |
| eq. (36)+A/$\kappa^5$ | 0.3667876(4) | −0.2302(1) |
| Table 1 | 0.3667875(2) | −0.23010(2) |

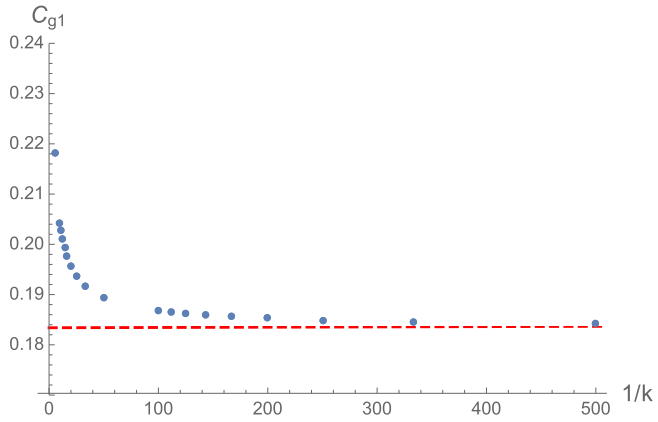


**Fig. 3.** Limit behavior for $C_{g_1}$ at close approach. $C_{g_1} \to C_1/2$ for $\kappa \to 0$.

the configurations of constant electrostatic potential on the two squares are, in particular, constant on a single square. Then, as the latter condition entails, in accordance with the Dirichlet principle, that the energy attains a minimum, i.e. $C_{g1} > C_1/2$, this implies that $C_g(\kappa) \geq C_1$ and, from (38), that $C_{g1}$ and, then, $C_g$ are growing functions of $\kappa$ near $\kappa = 0$. To our best knowledge the only known cases of computable behavior of $C_g$ for $\kappa \to 0$ are the case of two spheres (the result could be obtained from the coefficients computed in Ref. [3]) and the case of two disks, calculated in Refs. [5,6]. We pointed out in Refs. [4,6] that the short distance behavior depends both on the dimensionality of the *contact zone* and on the existence of a boundary.

The relevant analogy of the present study is with two parallel equal disks of radius $a$, where

$$C_{g_1} \underset{\kappa \to 0}{\to} a\left(\frac{1}{\pi} + \frac{\kappa}{2\pi^2}(\gamma_D - \log\kappa)\right) \tag{39}$$

with $\gamma_D = 1 + \log\pi \simeq 2.145$ and $C_1 = 2a/\pi$. The complete analytical result (39) was firstly derived in Ref. [20].

The term $\kappa\log\kappa$ in (39) is particularly important as it implies a logarithmic divergent repulsive force at short distances, as it is discussed more extensively in section 7. The physical origin of this term is explained considering the particular case of equal charges $Q_1 = Q_2 \equiv Q$. In this case the energy takes the form $W = Q^2/C_{g_1}$ and for continuity the solution of the Laplace equation for the system is approximated by the potential generated by the same charge distribution $\sigma_1(\mathbf{x})$ of the single conductor. The charge density is pushed toward the edges and, as a first approximation, the distribution near the edge can be taken as that given in (28). This distribution allows an easy direct computation of the force between the plates up to an additive constant. In the chosen configuration, $Q_1 = Q_2$, the second term in (11) is absent and the knowledge of $F$ at small $s$ (see Section 7) gives $C_{g_1}$ by integration of (11). Using $C_{g_1} = C_1/2$ for $\kappa = 0$ we have:

$$C_{g_1} = \frac{C_1}{2} + \kappa\left(\gamma_1 \log\frac{1}{\kappa} + \gamma_2\right) \tag{40}$$

where:

$$\gamma_1 = \frac{\pi}{2} C_1^2 \mathscr{P} \overline{b_\sigma^2} \tag{41}$$

with $\mathscr{P}$ the perimeter of the single plate and $b_\sigma$ is defined in (28).

The known analytical solution for a disk gives, for a unit charge, $b_\sigma = (\sqrt{2}/4\pi)a^{-3/2}$ and (41) reproduces the exact coefficient $1/2\pi^2$ of the logarithmic term in (39). The case of two squares is more complicated as the presence of corners produces a further charge concentration. In this case (41) has to be taken as a simplified model. Inserting the computed values of the parameters $C_1$ and $\overline{b_\sigma^2}$ we obtain the estimate $\gamma_1 \simeq 0.056(2)$, i.e.

$$C_{g_1} \simeq \frac{C_1}{2} + 0.056\kappa\left(\log\frac{1}{\kappa} + \text{cost.}\right) \tag{42}$$

The presence of the corners enhances the repulsive force then we expect that for squares we have a behavior like (40) but with $\gamma_1 > 0.056$. To test the analysis with our numerical results, let us consider

$$\frac{\delta C_{g_1}}{\kappa} = (C_{g_1} - C_1/2)/\kappa \tag{43}$$

We plot the data in Fig. 4 and the agreement is quite good. The dashed line is a fit of the form (40) and gives

$$\frac{\delta C_{g_1}}{\kappa} \simeq 0.061(2)\log\frac{1}{\kappa} + 0.060(5) \tag{44}$$

For the fit we used the distances $0.001 \leq \kappa \leq 0.05$. The points with $\kappa < 0.001$ are excluded from the fit for the reasons already discussed and it is expected that the corresponding points in Fig. 4 are underestimated. In our opinion, the data show that qualitatively two equal squares electrodes have the same behavior of two disks at short distances, and the simplified model (41) is fairly accurate. The implications of this result on the forces is discussed in section 7.

### 6.2. Mutual capacitance C at close approach

For the mutual capacitance $C$, to our best knowledge there are

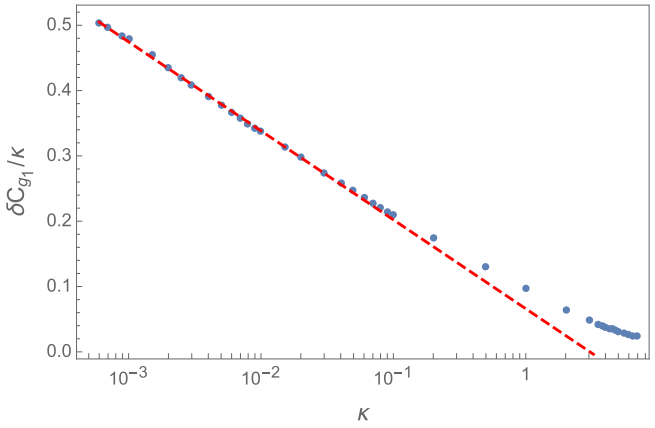


**Fig. 4.** The points represent our numerical results for the quantity $(C_{g_1} - C_1/2)/\kappa$ as a function of $\log\kappa$ The dashed line is the linear best fit in very good agreement with (42) for the small values of $\kappa$.

no exact results for the edge effects. The assumption of a uniform boundary, i.e. neglecting corners, leads to a Thomson-like approximation, see Ref. [21], which, for unit squares, reads

$$\begin{aligned} C &\simeq \frac{1}{4\pi\kappa} + \frac{1}{2\pi^2}\left\{1 + \log\left(1 + \frac{\pi}{\kappa} + \log\left(1 + \frac{\pi}{\kappa}\right)\right)\right\} \\ &\simeq \frac{1}{4\pi\kappa} - \frac{1}{2\pi^2}\log\kappa + \frac{1+\log\pi}{2\pi^2} \\ &= C_{geom} + 0.05066\log\frac{1}{\kappa} + 0.1086 \end{aligned} \tag{45}$$

Formula (45) is based on the extrapolation of the analysis of Thomson [22] for strips. A.E.H. Love has improved the formula for strips [23] leading to a change in the constant coefficient in (45). Love's results have been verified numerically in Ref. [24]. A more general formula for arbitrary shapes of the plates has been proposed by Soibel'man [25] and Kuester [26], leading again to a change in the constant coefficient in (45), 0.1086→0.1046.

The study of the edge effects $\delta C = C - C_{geom}$ is rather difficult. Below it is shown that the numerical computation supports the behavior suggested by (45)

$$\delta C = C - \frac{1}{4\pi\kappa} = a\log\kappa + b \tag{46}$$

but the *quantitative* verification of (45) is out of reach within the present numerical precision. Formulas (46) and (45) are expected to have corrections of order $\kappa\log^2\kappa$. For $\kappa = 10^{-3}$ the difference between the edge correction extracted from Table 2 and the prediction (45) is about 0.022, of the same order of $\kappa\log^2\kappa \sim 0.048$, this implies that the above corrections are not negligible in principle. Computations at smaller values of $\kappa$ are not reliable with our limitation on $N$ ($N_{max} \sim 460$). Then the quantitative conclusions are inevitably provisional in nature.

The results are summarized in Fig. 5. The line in the figure is a fit of the form (46), with

$$a = -0.044(3); \quad b = 0.140(5) \tag{47}$$

The result shows a small discrepancy with respect the value for $a$ in (45). On the other hand a fit with a fixed value $a = -1/2\pi^2$ and a further term of the form $c\kappa\log^2\kappa$ gives the dashed line in Fig. 5, $b = 0.096$ , $c = 0.054$. The value for $b$ is of the same order of the one predicted in (45). From the figure it is clear that within our precision we cannot distinguish between the two parametrizations then

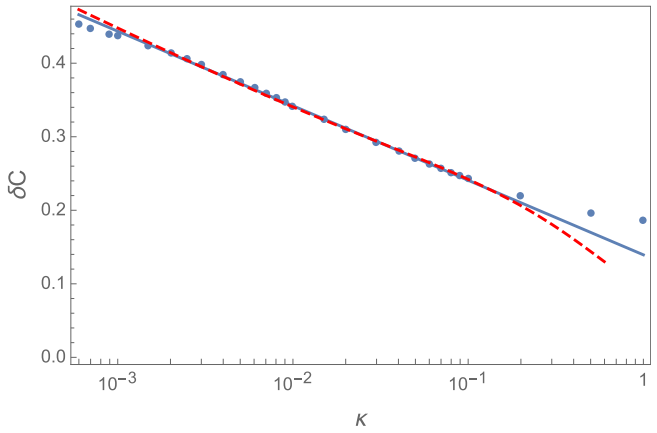


**Fig. 5.** $\delta C$ (see (46)) as a function of $\log\kappa$. The dashed line is Thomson approximation.

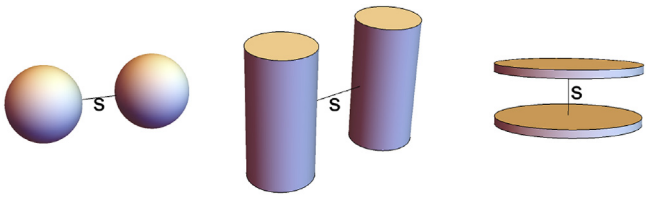


**Fig. 6.** Schematic diagram useful to visualize different kinds of contact zones.

we can not confidently confirm the value $a = -1/2\pi^2$.

Due to these difficulties a reasonable statement could be that only a computation at smaller $\kappa$'s with a larger $N$ or with an alternative method could brings to more definitive conclusions on the edge effects for $C$. This uncertainty does not effect the leading order behavior for forces, as discussed in the next section.

## 7. Forces

The general form of the force for two equal conductors is given in (11). To avoid misunderstandings let us stress the following point. The definition of the force as $-\nabla W$ is correct for isolated conductors, i.e. fixed charges. The expression (11) is anyhow valid *for any configuration of the conductors*, as, in principle, it depends only on the charge density distribution and on Coulomb's law. For isolated conductors, all the dependence on the distance is in the capacitances appearing in (11). In different configurations, for example with one or two fixed potentials, one has to express in equation (11) the charges through the potentials via (1) after taking the derivatives, i.e. the charges also depend on the distance. Here we discuss only the case of isolated conductors at short distances, other cases can be easily analysed using the form of $C_g$ and of $C$.

It can be useful to give a short summary of the main conclusions contained in Refs. [4,5] on the character of short distance forces, before presenting the results for the particular problem of equal squares. The generalization of (11), giving the component of the force along the direction of $s$ for two different conductors of arbitrary shapes and position in space is

$$F = \frac{1}{2}\frac{(Q_1+Q_2)^2}{(C_{g1}+C_{g2})^2}\frac{\partial}{\partial s}(C_{g1}+C_{g2}) - \frac{1}{2}\frac{\partial}{\partial s}\left[\frac{(C_{g2}Q_1 - C_{g1}Q_2)^2}{(C_{g1}+C_{g2})^2}\frac{1}{C}\right] \tag{48}$$

where

$$C_{g_1} = C_{11} + C_{12}; \quad C_{g_2} = C_{22} + C_{12}; \tag{49}$$

these quantities are both finite for $s\to 0$, $s$ being the distance between the conductors. The "global capacitance" of the system is $C_g = C_{g_1} + C_{g_2}$.

Let us start by discussing the second term in (48). The finiteness property of coefficients (49) implies that this term is dominated by the short distance behavior of $C$. In the general case $C$ diverges for $s\to 0$ and the degree of divergence is connected to the dimensionality of the contact zone between electrodes. With the term "contact zone" we mean the set of the points common to both electrodes when $s = 0$. (see Fig. 6).

We can take two spheres, two parallel cylinders and two parallel disks (or squares) as typical examples of dimensionality 0, 1, 2 respectively. In the three cases we have for the leading behavior in the region $s\to 0$

$$C^{(0)} \sim A^{(0)} \log\frac{1}{s}; C^{(1)} \sim \frac{A^{(1)}}{\sqrt{s}}; C^{(2)} \sim \frac{A^{(2)}}{s}$$

with $A$ a constant. The respective attractive contributions to (48) are, for $s \to 0$:

$$F^{(0)}_{attr} = -\frac{B^{(0)}_1}{s\log^2 s}; F^{(1)}_{attr} = -\frac{B^{(1)}_1}{2\sqrt{s}}; \quad F^{(2)}_{attr} = -B^{(2)}_1, \tag{50}$$

with

$$B^{(I)}_1 = \frac{1}{2A^{(I)}} \frac{\left(C_{g2}(0)Q_1 - C_{g1}(0)Q_2\right)^2}{\left(C_{g1}(0) + C_{g2}(0)\right)^2}. \tag{51}$$

It is apparent that while for point-like or line-like contact zones the force is attractive, and divergent, for planar contacts this part of the force is constant. In the last instance, which covers the case of two planar squares, the character of the force is determined by the first term in (48), which depends only on $C_g$. It has to be noted that the subleading terms in the expansion of $C$ for small $s$ are not relevant for (50), as anticipated in the previous sections.

Now let us consider the first term in (48). We have shown in section 6 that in our case $C_g$ is a growing function of $s$ and the proof extends trivially for a contact of two generic plates and we assume here that it is true also in the general case. One expect in a generic situation

$$C_g \sim C_g(0) + sB_2 \tag{52}$$

This gives a constant repulsive contribution to (48) and the total force is, for a 2-d contact zone

$$F = \frac{1}{2}\frac{(Q_1+Q_2)^2}{C_g(0)^2}B_2 - B_1 \tag{53}$$

The sign of the force depends from the system and on the charge ratio $Q_1/Q_2$. This general description fails to describe the case of two equal disks (and of two equal squares as will be shown below). The physical reason is the following. The nature of the first term in (48) is most easily seen by considering the case of equal conductors and equal charges, in this case the second term in (11) vanishes. The like charges in the conductors tend to repel each other but the zero thickness prevents displacements along the $z$ axis and the charges are pushed to the edges. In the case of equal disks, or in general for two equal planar electrodes, the diverging charge density at the boundary produces a divergent logarithmic force, clearly repulsive. This has been shown analytically for disks in Refs. [4,5] and will be verified numerically below for squares.

The order of magnitude of the effect has been illustrated in (40) and (41) and the argument goes as follows. Let $\Phi(\mathbf{x})$ be the electrostatic potential of a *single* equipotential plate. In a system of two plates at small distance $z$, with respect to a typical dimension, the second plate is still an equipotential surface for $\Phi$ up to corrections of order $z$. The general form of the potential near an edge is (see problems in §3 of [19])

$$\Phi = A_1 - A_2\sqrt{\rho - \xi} \tag{54}$$

where $\xi$ is the distance from the edge and $\rho^2 = \xi^2 + z^2$. The constant $A_2$ is related to the behavior of the charge density near the edge:

$$2\pi\sigma = -\partial_z\Phi\big|_{z=0} = \frac{A_2}{\sqrt{2\xi}}$$

i.e.

$$\sigma \simeq \sqrt{2}\,\frac{A_2}{4\pi}\frac{1}{\sqrt{\xi}} \equiv b_\sigma \frac{1}{\sqrt{\xi}}. \tag{55}$$

The approximation (55) is valid up to a certain distance $\lambda$ from the edge, and $\lambda$, by its definition, depends only on the single plate, not on $z$. In the same approximation the electric field along the $z$ axis is given by

$$E = -\partial_z\Phi \simeq \frac{A_2}{\sqrt{2}}\sqrt{\xi}\,\frac{1}{\sqrt{\xi^2+z^2}}$$

The force per unit length exerted by a plate due to this divergent contribution is then

$$f = \int_0^\lambda dx\sigma E \simeq \frac{A_2^2}{4\pi}\log\frac{\lambda}{z} = 2\pi b_\sigma^2 \log\frac{\lambda}{z}.$$

The total force is obtained by integration on the boundary, the constant $A_2$ in general depends on the point considered:

$$F = \oint f d\ell = 2\pi\mathscr{P}\overline{b_\sigma^2}\log\frac{1}{z} + \text{cost} \tag{56}$$

where $\mathscr{P}$ is the perimeter and $\overline{b_\sigma^2}$ is the mean value on the boundary. For a uniform boundary, as for a disk or for a square neglecting corners, $A_2$ is independent on the point on the boundary.

For two unit charges and $z \to 0$, from (11)

$$F = -\frac{1}{C_{g_1}(0)^2}\partial_z C_{g_1} = -\frac{4}{C_1^2}\partial_z C_{g_1}. \tag{57}$$

By integration we can obtain $C_{g_1}(z)$ and comparing with (40) we obtain the estimation (41).

In realistic situations the finite thickness or the non perfect identity of the conductors can smooth the logarithmic divergence to a constant force of the type (53). These effects for nearly flat conductors have a typical scale $\delta$ (the thickness or the difference in sizes for disks or squares) small with respect the typical scale $L$ of the system. For continuity reasons we expect that in the region $\delta \ll s \ll L$ the logarithmic behavior is a good approximation. This has been explicitly verified for disks of different sizes in Ref. [5].

It is worth to note that even for a logarithmic divergent force the energy is finite for $s \to 0$, i.e. the work needed to bring together the two plates is finite:

$$W = \frac{1}{4}\frac{(Q_1+Q_2)^2}{C_{g_1}(0)} = \frac{1}{2}\frac{(Q_1+Q_2)^2}{C_1}.$$

Before closing this long parenthesis on the general aspects of the problem let us mention another particular case. When two conductors touch they acquire the same potential and charges in the ratio $Q_1/Q_2 = C_{g_2}(0)/C_{g_1}(0)$. $C$ in any case diverges as $s \to 0$ and the second term in (48) is the derivative of a term which vanishes more rapidly than $s$, then goes to zero as $s \to 0$. The resulting total force is repulsive if $C_g$ grows with $s$. This has been also pointed out in the particular case of two spheres in Ref. [3].

In the case at hand the force at short distances, using (11), (40) and $L = 1$, is given by

$$F = \frac{(Q_1+Q_2)^2}{C_1^2}\left(\gamma_1 \log\frac{1}{k} + \gamma_2 - \gamma_1\right) - \frac{\pi}{2}(Q_1-Q_2)^2. \tag{58}$$

The second term in (58) is due to the leading term $C$ for $\kappa \to 0$. Edge corrections contribute only at order $\kappa$ in the force, as can be checked from (46). Inserting the fitted numerical values:

$$F \simeq (Q_1+Q_2)^2\left(0.45(2)\log\frac{1}{\kappa} - 0.01(2)\right) - \frac{\pi}{2}(Q_1-Q_2)^2 \tag{59}$$

Equation (58) exhibits the announced logarithmic divergent force. It is repulsive for any choice of the charges and then also for charge of opposite sign, with the exception of $Q_1 = -Q_2$.

To help the reader in the visualization of the mechanism giving rise to (58) we give in Fig. 7 the trend of charge density near the edge of the square. The squares are parallel to $x, y$ plane and the coordinates are chosen between $-L/2, +L/2$ with $L = 1$. In the figure are shown the charge density $\sigma_1$ for a single square (i.e. in the computation of $C_1$) and the charge density $\sigma(x)$ in the case of two squares at kept at the same potential and $\kappa = 0.001$, both on the midline of the square. The line is the fit (29). It is apparent that the two distribution are practically identical, supporting the model behind (41).

For comparison it is also reported the charge distribution in the case of two oppositely charged squares ($Q = \pm 1$) at the same distance, here $\sigma \simeq 1$ (omitting edge effects).

By elementary arguments a constant charge density, with opposite signs on the squares, gives rise to an attractive force

$$F_{attr} = -2\pi$$

for unit charges on the plates, this is exactly the attractive contribution (second term) in (58) for $Q_1 = -Q_2 = 1$.

The logarithmic singularity parallels the analogous behavior for disks [4,5] and by analogy it is expected to be smoothed toward a constant force when the plates are not equal or if the thickness is introduced, as explained above. This point deserves further studies in the case of squares.

## 8. Conclusions

This work presents a numerical and semi-analytical study of the electrostatic problem for two equal squares. Extensive computations with the BEM method give definite results for the large distance regime and bring some light for small distances between the electrodes. In the first case it is verified that from knowledge of capacitance coefficients some parameters relative to single conductors can be deduced: the self-capacitance and the quadrupole moment. In the small distance region it has been verified a close parallelism with the behavior of circular electrodes: a logarithmic repulsive force appears. This evidence confirms the thesis exposed in previous works about the dependence of the forces on the dimensionality of the contact region between electrodes. In realistic situations some corrections are expected but it is clear that this peculiar electrostatic effect must be taken into account in experiments involving precision measurement of forces at short distances.

The presence of a short-distance repulsive force has some evident phenomenological implications, as, for example, the presence of a stable oscillation along $z$ axis. This is surely there for opposite charged electrodes and, for suitable charge ratios, can also appear for even charged conductors. The studies on the properties of electrostatic forces for spheres [3] and disks [4,5] suggest that the subject can be relevant in the field of nano-scale physics, surface interactions and precision physics experiments.

On the theoretical side, for the specific problem of two equal squares, the main problem remains the exact form of the leading edge correction for the mutual capacitance $C$: the numerical computation is unable to confirm the exact coefficients in the Thomson approximation.

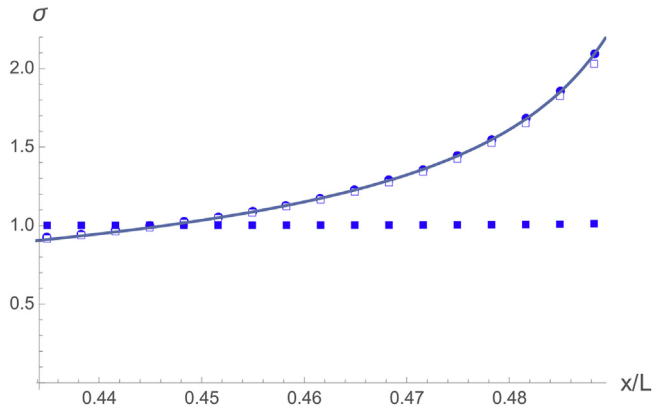


**Fig. 7.** Charge distribution for a single square (filled disks) and for a couple of squares kept at the same potential (empty squares). The line is the fit (29). Filled squares show the charge density for oppositely charged squares. The edge is located at $x = L/2$.

## Appendix A. Matrix element

We give here the explicit expression for $\tilde{K}_{ij}$ in the case of two parallel rectangular subareas $S_i, S_j$, in the plane $z = 0$ and $z$ respectively. The squared distance between two arbitrary points $(X_1, Y_1) \in S_i$ and $(X_2, Y_2) \in S_j$ is

$$d^2 = (X_1 - X_2)^2 + (Y_1 - Y_2)^2 + z^2$$

The dimensions of a cell are $(2dx_i, 2dy_i)$ and the area $A_i = 4dx_i dy_i$. Denoting with $(x_1, y_1)$ and $(x_2, y_2)$ the centres and by $\xi, \eta$ the offsets with respect to these points:

$$X_1 = x_1 + \xi_1; X_2 = x_2 + \xi_2$$
$$Y_1 = y_1 + \eta_1; Y_2 = y_2 + \eta_2$$

$d^2$ take the form

$$d^2 = (x + \xi_1 - \xi_2)^2 + (y + \eta_1 - \eta_2)^2 + z^2$$

where

$$x = x_1 - x_2; \quad y = y_1 - y_2$$

and

$$-dx_i \le \xi_1 \le dx_i; \quad -dy_i \le \eta_1 \le dy_i$$
$$-dx_j \le \xi_2 \le dx_j; \quad -dy_j \le \eta_2 \le dy_j$$

The matrix element $\tilde{K}_{ij}$ is

$$\tilde{K}_{ij} = \int_{-dx_i}^{dx_i} d\xi_1 \int_{-dx_j}^{dx_j} d\xi_2 \int_{-dy_i}^{dy_i} d\eta_1 \int_{-dy_j}^{dy_j} d\eta_2 \frac{1}{\sqrt{(x+\xi_1-\xi_2)^2 + (y+\eta_1-\eta_2)^2 + z^2}}$$

The integral can be performed with the result

$$
\begin{aligned}
K^{\sim}{}_{ij} &= f_3(x+dx_j,y,z) - f_3(x-dx_j,y,z) f_3(x,y,z) \\
&= f_2\left(x,y+dy_j,z\right) - f_2\left(x,y-dy_j,z\right) f_2(x,y,z) \\
&= f_1(x+dx_i,y,z) - f_1(x-dx_i,y,z) f_1(x,y,z) \\
&= f_0(x,y+dy_i,z) - f_0(x,y-dy_i,z)
\end{aligned} \tag{A.4}
$$

where

$$
\begin{aligned}
f_0(x,y,z) = \frac{1}{12}\Big\{ & -3x^3 - 2\left(x^2+y^2+z^2\right)^{3/2} + \\
& 6z^2\sqrt{x^2+y^2+z^2} - 12xyz\tan^{-1}\left(\frac{xy}{z\sqrt{x^2+y^2+z^2}}\right) \\
& -3x^2y - 9xy^2 + 12xyz\tan^{-1}\left(\frac{y}{z}\right) \\
& -3xz^2 - y^3 - 3yz^2\Big\} \\
& +\frac{1}{2}x^2y\log\left(\sqrt{x^2+y^2+z^2}+y\right) \\
& +\frac{1}{2}x\left(y^2-z^2\right)\log\left(\sqrt{x^2+y^2+z^2}+x\right) \\
& +\frac{1}{2}yz^2\log\left(\sqrt{x^2+y^2+z^2}-y\right)
\end{aligned}
$$

For coplanar cells we have to take the limit $z \to 0$ of the previous result and the function $f_0$ takes the form

$$
\begin{aligned}
f_0(x,y) = \frac{1}{4}\Big\{ & \left(2x^2y\log\left(\sqrt{x^2+y^2}+y\right)\right. \\
& +2x\left(x^2+y^2\right)\log\left(\sqrt{x^2+y^2}+x\right) \\
& +x\left(-x^2-y^2\right) - \frac{2}{3}\left(x^2+y^2\right)^{3/2} \\
& -x^2y - 2x^3\log\left(\sqrt{x^2+y^2}+x\right) - 2xy^2 - \frac{y^3}{3}\Big\}
\end{aligned}
$$

## References


[1] J. Lekner, Electrostatic force between two conducting spheres at constant potential difference, J. Appl. Phys. 111 (7) (2012) 076102.
[2] A.S. Khair, Electrostatic forces on two almost touching nonspherical charged conductors, J. Appl. Phys. 114 (13) (2013) 134906.
[3] J. Lekner, Electrostatics of two charged conducting spheres, Proc. R. Soc. A (2012) rspa20120133.
[4] F. Maccarrone, G. Paffuti, Some comments on the electrostatic forces between circular electrodes, J. Electrost. 84 (2016) 135–142.
[5] G. Paffuti, Numerical and analytical results for the two disks capacitor problem, Proc. R. Soc. A 473 (2017) 20160792.
[6] G. Paffuti, E. Cataldo, A. Di Lieto, F. Maccarrone, Circular plate capacitor with different discs, Proc. R. Soc. A 472 (2016) 20160574.
[7] F. Maccarrone, G. Paffuti, Capacitance and potential coefficients at large distances, J. Electrost. 83 (2016) 22–27.
[8] R.F. Harrington, J.L. Harrington, Field Computation by Moment Methods, Oxford University Press, 1996.
[9] J.T. Katsikadelis, Boundary Elements: Theory and Applications, Elsevier, 2016.
[10] C.-O. Hwang, M. Mascagni, Electrical capacitance of the unit cube, J. Appl. Phys. 95 (7) (2004) 3798–3802.
[11] F.H. Read, N.J. Bowring, The cpo programs and the bem for charged particle optics, Nucl. Instrum. Meth. Phys. Res. Sect. A 645 (1) (2011) 273–277.
[12] F. Read, Improved extrapolation technique in the boundary element method to find the capacitances of the unit square and cube, J. Comput. Phys. 133 (1) (1997) 1–5.
[13] S. Rao, A. Glisson, D. Wilton, B. Vidula, A simple numerical solution procedure for statics problems involving arbitrary-shaped surfaces, IEEE Trans. Antenn. Propag. 27 (5) (1979) 604–608.
[14] D.K. Reitan, Accurate determination of the capacitance of rectangular parallel-plate capacitors, J. Appl. Phys. 30 (2) (1959) 172–176.
[15] F. Read, Capacitances and singularities of the unit triangle, square, tetrahedron and cube, COMPEL 23 (2) (2004) 572–578.
[16] H. Nishiyama, M. Nakamura, Form and capacitance of parallel-plate capacitors, IEEE Trans. Compon. Packag. Manuf. Technol. Part A 17 (3) (1994) 477–484.
[17] E. Goto, Y. Shi, N. Yoshida, Extrapolated surface charge method for capacity calculation of polygons and polyhedra, J. Comput. Phys. 100 (1) (1992) 105–115.
[18] F. Read, Improved extrapolation technique in the boundary element method to find the capacitances of the unit square and cube, J. Comput. Phys. 133 (1) (1997) 1–5.
[19] L. Landau, E. Lifshitz, Electrodynamics of Continuous Media, §3, Pergamon Press, Oxford, 1984.
[20] C. Atkinson, F. Leppington, The asymptotic solution of some integral equations, IMA J. Appl. Math. 31 (3) (1983) 169–182.
[21] A.H. Scott, H. Curtis, Edge correction in the determination of dielectric constant, J. Res. (1939) 747–775.
[22] J.J. Thomson, Notes on Recent Researches in Electricity and Magnetism: Intended as a Sequel to Professor Clerk-Maxwell's Treatise on Electricity and Magnetism, Clarendon Press, 1893.
[23] A.E.H. Love, Some electrostatic distributions in two dimensions, Proc. Lond. Math. Soc. 2 (1) (1924) 337–369.
[24] H. Wintle, S. Kurylowicz, Edge corrections for strip and disc capacitors, IEEE Trans. Instrum. Meas. 1001 (1) (1985) 41–47.
[25] Y.S. Soibel'man, Asymptotics of the capacity of a condenser with plates of an arbitrary shape, Sib. Math. J. 25 (6) (1984) 966–978.
[26] E.F. Kuester, Explicit approximations for the static capacitance of a microstrip patch of arbitrary shape, J. Electromagn. Waves Appl. 2 (1) (1988) 103–135.